ALLEGATO 2

Elenchi domande Colloquio:

Raggruppamenti: 1^ domanda: idrologia forestale, monitoraggio idrologico ed idraulico, tecniche analitiche di spettroscopia laser e di cromatografia ionica

Raggruppamenti: 2^ domanda: metodi di gestione della sicurezza di laboratorio chimico e di sistemi di qualità accreditati, regolamento per la disciplina, l'accesso e l'uso delle attrezzature e degli spazi destinati ad attività di ricerca

1^ terna:

1a-Nell'ambito dell'idrologia forestale, si chiede di spiegare quale strumento può essere usato per la misura dell'intensità di precipitazione e come avviene il campionamento ed analisi di laboratorio della precipitazione per la determinazione della sua composizione isotopica (^2H e ^{18}O).

2a-Si indichino i dispositivi di sicurezza individuali da adottare in laboratorio per la determinazione della concentrazione in ioni maggiori nelle acque.

3a-In Microsoft Excel, cosa indica "B1:B22"?

2^ terna

1b-Nell'ambito dell'idrologia forestale, si chiede di spiegare quali strumenti possono essere usati per la misura del livello idrometrico in piccoli torrenti montani e come avviene il campionamento ed analisi di laboratorio dell'acqua di torrente per la determinazione delle concentrazioni in ioni maggiori.

2b-Si indichino i dispositivi di sicurezza individuali da adottare in laboratorio per la determinazione della composizione isotopica delle acque (^2H e ^{18}O).

3b-In Microsoft Word, cosa vuol dire cancellare la formattazione di una sezione di un documento?

A Rationale for Old Water Discharge Through Macropores in a Steep, Humid Catchment

JEFFREY J. McDONNELL

Watershed Science Unit, Department of Forest Resources, Utah State University, Logan

Simultaneous observations of rapid preferential flow through macropores and isotopically "old" water displacement remain unresolved in the Maimai (M8) catchment. Continuous, three-dimensional soil moisture energy conditions were monitored in two discrete catchment positions for a series of storm events in 1987. Tensiometric response was related to the soil water characteristic curve, hillslope throughflow, and total catchment runoff. For events yielding ≪2 mm hr^{-1} peak runoff, near-stream valley bottom groundwater systems discharged water volumes sufficient to account for storm period streamflow. This process was assisted by regular low (<−40 cm H$_2$O) matric potential conditions and rapid filling of available soil water storage. For events yielding >2 mm hr^{-1} peak storm flow, hillslope hollow drainage into steeply sloping first-order channels dominated old water production and most of the catchment storm flow. Highly transient macropore-driven processes of crack infiltration (bypass flow), slope water table development, and lateral pipe flow enabled large volumes of stored water to be delivered to the first-order channel bank at the appropriate time to satisfy catchment storm flow volumes and water isotopic and chemical composition.

1. INTRODUCTION

Progress in understanding processes of storm runoff generation in humid headwater catchments is hampered by discrepancies often found between physical, chemical, and isotopic approaches. Furthermore, the results from chemical and natural isotope separations of stream water into old (pre event) and new (event) water sources often appear to contradict results from hydrometric studies of pathways of water movement on hillslopes.

Recent work in a highly responsive catchment at Maimai (M8) on the west coast of New Zealand has yielded conflicting results regarding the importance of new versus old water in through-flow transmission. Hydrometric studies employing dye tracing and subsurface flow measurement [*Mosley*, 1979, 1982] concluded that rapid flow of new water through macropores was capable of accounting for storm period streamflow. In more recent natural stable isotope and chemical tracing studies, *Pearce et al.* [1986] and *Sklash et al.* [1986] explicitly refuted this earlier interpretation by indicating that old water dominated throughflow in all storm events monitored. On the basis of previous computer simulations [*Sklash and Farvolden*, 1979] and physical principles [*Gillham*, 1984], they suggested that a rapid matrix flow displacement mechanism, occurred through (1) saturated wedges on the lower slopes and (2) groundwater ridges in the valley bottoms. This process involved capillary fringe response [*Ragan*, 1968], which increased local hydraulic gradients and promoted increased gravity drainage of old water to the stream channel.

For this study area it now appears that there may be no need for rapid macropore flow transport of new water to explain the subsurface transmission of water downslope, because stored water is discharged into the stream channel. However, the capillary fringe effect, which limits storage and enables rapid discharge of stored water, has only been clearly demonstrated in laboratory models [*Abdul and Gill-*

ham, 1984; *Stauffer and Dracos*, 1986] and mathematical simulations but has not been well documented in the field. The applicability of these physical and mathematical models to real hillslopes and field soils may be questionable given the latter's heterogeneity.

This paper describes the soil moisture energy conditions at different topographic positions within the M8 catchment and explains the process of rapid exfiltration of isotopically old water into a channel during rainfall events. In companion papers, *McDonnell et al.* [1990], and M. K. Stewart and J. J. McDonnell (Modeling water flow in soils of a steep headwater catchment traced by deuterium, submitted to *Water Resources Research*, 1990 (hereinafter referred to as M. K. Stewart and J. J. McDonnell, 1990)) treat the isotopic behavior of the rainfall, soil water, and channel storm flow.

2. STUDY AREA AND METHODOLOGY

The study was carried out in the Maimai M8 catchment (Figure 1), located in the Tawhai State Forest (45°05'S, 171°48'E), North Westland, New Zealand, described by *Pearce et al.* [1976]. Mean annual gross rainfall in the study area is approximately 2600 mm, producing approximately 1550 mm of runoff from 1950 mm of net rainfall [*Rowe*, 1979]. *Pearce and McKerchar* [1979] note that the catchments are highly responsive to storm rainfall, with 1000 mm (65%) of the mean annual runoff and 39% of the total annual rainfall (*P*) in the form of quickflow (*QF*), as defined by *Hewlett and Hibbert*'s [1967] separation method.

The M8 catchment is underlain by a firmly compacted, moderately weathered, early Pleistocene conglomerate known as the Old Man Gravels. This unit has been described as "effectively impermeable" [*Mosley*, 1979, p. 795], and hydrogeological investigations by D. Bell (personal communication, 1989) indicate that the upper 20 m of this unit form an impermeable capping to the lower conglomerate aquifer systems, with permeabilities and transmissivities of the order of <0.3 m d^{-1} and <15 m^2 d^{-1}, respectively. Slopes are short (<30 m) and steep (mean 34°), with a local relief of 100–150 m. Catchment side slopes consist of regular spurs of
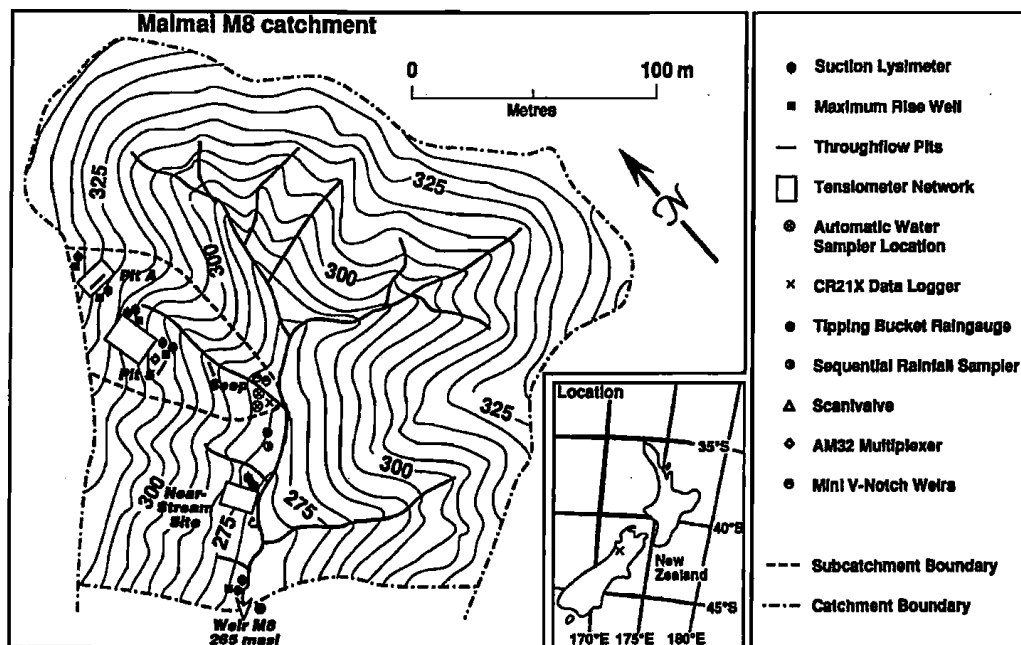
Fig. 1. M8 catchment showing locations of hydrometric instrumentation and sampling sites.

Old Man Gravel bedrock and linear hollows infilled with matrix-rich colluvium. Soils in the catchment have developed from the underlying soft, weathered conglomerate and colluvium and are broadly classified as Blackball Hill soils [New Zealand Soil Bureau, 1968; Mew et al., 1975]. They show large spatial variability in depth (mean 0.6 m, range 0.2–1.8 m) and character (from podsolized yellow brown earth (YBE), to mottled YBE, to gley soils) and are dominantly stoney throughout their profiles. Mineral soil horizons are overlain by a thick (mean 170 mm) well-developed upper humic horizon. Webster [1977] reported average infiltration capacity of the humic layer and average saturated hydraulic conductivity (K_{sat}) (measured from field cores in the laboratory) of the upper mineral soil of the order of 6100 and 250 mm hr^{-1}, respectively. Limited field measurements of field-saturated hydraulic conductivity (K_{fsat}), using a Guelph permeameter [McDonnell, 1989], suggest that conductivity values are highly variable and may range from ≪5 mm hr^{-1} in poorly drained hollows to the 250 mm hr^{-1} value reported by Webster on well-drained nose slopes.

The experimental design of M8 (3.8 ha) and an intensively instrumented subwatershed (0.3 ha) have been fully documented [Pearce et al., 1986] and include a complete hydrometric recording system along with eight hillslope through-flow pits located in a variety of soil depth and topographic positions on the slope (Figure 1). Three zones within M8 were intensively sampled and instrumented during September–December 1987 [McDonnell, 1989]. The Pit A site (not discussed in this paper) included the deployment of a vertical and horizontal array of 24 recording tensiometers (Scani-valve Model W0602/1P-24T 24 position fluid scanning switch, Sensym SCX15DN pressure transducer) to characterize unsaturated zone response characteristics in an up-slope zone known to produce large-event water contributions. The Pit 5 site consisted of an electronically multiplexed and logged array of 32 tensiometers (Campbell 21X logger, Sensym SCX15DN pressure transducers) in a

midslope zone to assess the effect of the capillary fringe on saturated wedge development and moisture potentials. The near-stream site was located in a near-stream valley bottom zone and included the same monitoring equipment as Site A, installed along transects both lateral and normal to the channel. The purpose of this site was to monitor the effect of the capillary fringe on near-stream groundwater ridging behavior. Details of tensiometer design and performance are given by J. J. McDonnell (Electronic versus fluid multiplexing in recording tensiometer systems, submitted to Hydrological Science and Technology, 1990). Laboratory calibrations of tensiometer tubing pressure response were conducted for a series of tubing materials, diameters, and lengths. Tube material was chosen to maintain negligible pressure attenuation downline.

In addition to hydrometric recording, streamflow, through flow, groundwater, soil water, and precipitation were sampled automatically (Automatic Liquid Sampler 4BSEC) and manually to enable isotopic (deuterium) and chemical (chloride, electrical conductivity) separation of event and pre event water components in storm runoff. Soils were sampled at the near-stream, Pit 5 and Pit A sites. In each case, samples were biased toward stone-free and root-free portions of the horizon because of sampling difficulty. Much of the profile at each site was stoney, and therefore proper undisturbed cores were difficult to extract. Horizon boundaries at each site were distinct, and the Old Man Gravel surface formed an impermeable underlying layer. Table 1 lists the average bulk density and porosity values obtained from each zone, and Figure 2 shows averaged moisture release curves from three replicate cores at each sit, determined using a laboratory tension table apparatus.

3. MINERAL SOIL MACROPORES AND PREFERENTIAL FLOW

The definition of macropore size classes is quite arbitrary and does not necessarily relate to flow processes [Beven and

TABLE 1. M8 Soil Properties for Cores Taken in Three Slope Positions

Site	Total Soil Depth,* m	Sampling Depth, m	BD, g cm⁻³	θ %	Slope, deg	Topo-graphic Position
Pit A	0.6	0.25	1.5	43	40	upslope hollow
Pit 5	1.5	0.7	0.9	68	34	midslope hollow
Near stream	0.5	0.35	1.3	52	15	valley bottom

*At pit face.

Germann, 1982]. *Luxmoore* [1981] designated three size classes for pores: macro (>1000 μm), meso (10–1000 μm) and micro (<10 μm), where the micropore class corresponds to the soil matrix. In addition to pore size, however, pore structure (including continuity and connectivity) is also of crucial importance to the effective definition of a macropore [*Bouma*, 1981]. As a result, terms such as preferential pathways or macrochannels have been suggested to emphasize the importance of structure on flow dynamics. *Bouma et al.* [1977] have shown that different numbers and sizes of macropores may be effective under different conditions. Therefore a relevant definition of macropores for solute infiltration in a ploughed field may differ from a relevant definition for subsurface flow in a steeply sloping hillslope.

Mosley [1979, 1982] identified preferential flow paths at vertical pit faces in the Maimai catchments for a number of dyed water injection experiments. Assuming that the vertical faces are acceptable samples of the whole soil profile, Mosley's observations show that there are preferred pathways for flow, that is, along cracks and holes in the soil and along live and dead roots and root channels (macropores). In this study, only those pores which are hydrologically effective in terms of channeling flow through the soil and contributing to rapid subsurface flow are of principal concern.

Local M8 catchment conditions are different from many other areas where macropores have been identified because (1) the soil mass is steeply sloping (average 25°–45°), (2) the soil is shallow (average 0.6 m) and underlain by impermeable bedrock, (3) the soil profile is drained at its base by a

Fig. 2. Moisture release characteristics for soils in the near-stream, Pit 5 and Pit A locations.

continuous piping system, and (4) soils remain within 10% of saturation for most of the year. As a result of these conditions, the most hydrologically important macropore types in M8 are considered to be continuous pipes and cracks. The dependence of flow rate on the fourth power of the pore radius means that while the presence of these cracks and pipes may make only a very minor contribution to the total soil porosity, nearly all the rapid flow (at or near saturation) is through these channels [*Bouma and Anderson*, 1973; *Scotter*, 1978].

3.1. Pipes and Pipe Flow

Evidence from a number of recent field monitoring programs, particularly in the United Kingdom, has shown that pipe flow can be a substantial contributor to storm quick flow [*Jones*, 1979; *McCaig*, 1983; *Wilson and Smart*, 1984; *Jones*, 1987]. In the M8 catchment, pipes occur at the mineral soil-Old Man Gravel interface and extend laterally downslope over distances of several tens of meters [*Mosley*, 1979]. This conclusion is supported by the visual observations in this study of pipe outflows at pit faces along the banks of first-order channels and by the fact that hillslope runoff increases rapidly in a downslope direction. Conditions that promote pipe development in the M8 catchment seem to relate to (1) shallow soil depth, (2) underlying impermeable bedrock, and (3) root growth and decay.

Large roots extend vertically through the shallow mineral soil (average 0.6 m depth) but cannot penetrate the underlying conglomerate. Roots then extend laterally over the conglomerate surface (P. Tonkin, personal communication, 1988) for up to several meters. A. Watson (unpublished data, 1988), has shown that the maximum lateral length of 25-year-old *Pinus radiata* root systems in Mangatu Forest, North Island, New Zealand, is 10.4 m. Pipes formed by root growth and subsequent decay may be enlarged by eluviation. Conditions promoting this process in the M8 catchment would include high rainfall, rapid movement of infiltrating water to depth (discussed below), steep slopes and high hydraulic gradients, potentially dispersive soil at the mineral soil base, and the presence of pipe outlets at the first-order channel bank.

As a result of root decay and pore enlargement, a well-connected pipe network has become established in M8, which conducts a large percentage of subsurface storm flow. From limited visual observations at pit faces and along first-order stream banks, pipe outlets range from 3 to 100 mm in diameter.

3.2. Cracks and Bypass Flow

In well-structured soils like the clay-rich mottled and gleyed soils in the M8 hollows, flow through continuous cracks, described as channeling [*Beven*, 1981], short circuiting [*Bouma et al.*, 1981], or bypassing [*Smettem et al.*, 1983; *Van Stiphout et al.*, 1987], may result in a deeper penetration of rainfall and solutes than is predicted by uniform displacement [*Thomas et al.*, 1978]. The term "bypass flow" will be used in this paper to describe the vertical movement of free water along continuous cracks (from the mineral soil surface to its base) through an unsaturated or partially saturated soil matrix.

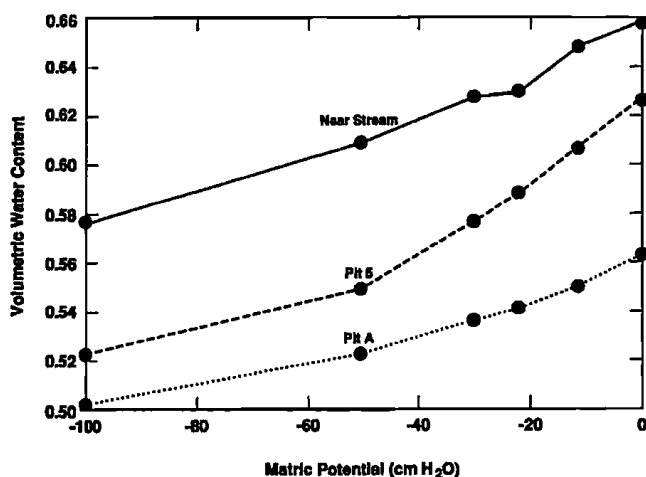The occurrence and rate of bypass flow will be determined

by (1) total rainfall depth and intensities, (2) prestorm soil moisture content, and (3) soil hydraulic conductivity (K). Bypass flow is a two-domain flow process whereby water movement in vertical cracks is driven by gravity, independent of flow in the soil matrix, which is driven by both gravity and matric (especially capillary) forces [*Germann*, 1986].

At the Pit 5 hollow site, for example, soil was excavated upslope from the pit face to identify any vertical cracking. Regularly spaced vertical cracks, roughly 1–3 mm wide, were observed extending from the mineral soil surface to the Old Man Gravel interface. These cracks showed signs of organic staining along their walls and fine "hairlike" root structures along their entire length. This evidence, together with dye tracer experimental results [*McDonnell*, 1989], suggests that water regularly moves through these channels. Maimai soils, while never dropping significantly below 90% saturation, do occasionally encounter dry periods (of about 3 weeks), when surface cracking can occur (P. Tonkin, personal communication, 1988). In many hillslope hollow zones, upper mineral soils are organic-rich, particularly their midslope sections. Mineral soil surfaces in some situations develop hydrophobicity, which increases the susceptibility to surface cracking.

4. RESULTS OF TENSIOMETRIC STUDIES

Tensiometer porous cups were embedded in the soil matrix (away from cracks and pipes) and are assumed to provide information on soil matrix conditions only. By combining the soil water potential data with storm rainfall, streamflow, and hillslope discharge, inferences may be made regarding the nature of subsurface flow. Soil physics considerations are aimed at identifying the rate of development and longevity of the water table, hydraulic gradients, and resulting subsurface water movement. Preferential flow in cracks and pipes, while not directly related to tensiometric response to storm rainfall, can be inferred from soil profile wetting patterns and hillslope discharge.

4.1. Near-Stream Response

Tensiometer numbers and porous cup depths for selected tensiometers in the near-stream location are shown in Figure 3. Site numbers are also shown and will be referred to in the following discussion on tensiometric response to storm rainfall. Fifty-eight millimeters of precipitation (P) fell during two short intense bursts on October 29, with peak 10 min intensities of the order of 14 mm hr^{-1}. Streamflow response was rapid, and peak specific discharge was 2.8 mm hr^{-1} (Figure 4). Thirty millimeters of runoff was produced, 29 mm of which was in the form of quick flow (QF). Antecedent precipitation indicies (API$_7$ and API$_{14}$, representing 7 and 14 days) were defined by API$_x = \Sigma_{i=1}^x Pi/i$, where Pi is the total gross precipitation on the ith day beforehand. API$_7$ and API$_{14}$ were relatively high (4.7 and 5.0 mm, respectively), and QF/P was 50%. The stream hydrograph had fully recovered from a preceding event on October 24, and base flow conditions were maintained prior to rain input. Pit A through-flow response mirrored that of the main channel and produced a peak discharge of 1250 ml min^{-1}. Seep discharge peaked 3.5 hours after both Pit A and the main channel. Peak flow was only 12.5 ml min^{-1}, and the hydrograph shape showed an extremely steep rise and recession.
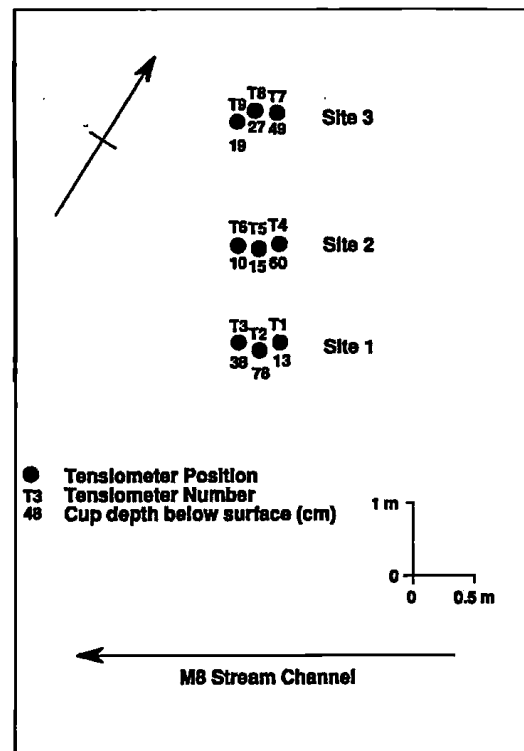

Fig. 3. Tensiometer location and porous cup depths for the near-stream site.

Tensiometric response in the near-stream zone was rapid throughout the soil profile. Soil water potential (ψ) is plotted as a continuous function of time for sites 1–3 (Figure 4). Prestorm ψ ranged from −45 to 10 cm H$_2$O, with average prestorm suction of about −30 cm H$_2$O. At sites 1, 2, and 3 all tensiometers responded at the same time (with no appreciable lag with depth) but about 6 hours after the start of the storm (Figures 4b–4d). In this case, about 90% of the total ψ shift occurred in response to the first rainfall burst at 2400 LT on October 28.

Peak tensiometric response coincided with the stream hydrograph peak. Once peak ψ values were reached, approximately constant values persisted at site 1 and near the surface at site 2 (T6), while the rest gradually declined. Some variation in ψ recession can be seen in Figure 4b, where the upslope site 3 tensiometers (T7–T9) showed a more rapid decline from peak positive ψ (0–20 cm H$_2$O) to negative ψ. Similarly, site 2 ψ recession was more rapid than site 1 ψ recession.

A plot of ψ versus soil depth of T1–T9 provides some indication of the infiltration-groundwater relationship. For t_0, t_1, t_2, and t_3, representing 2330 LT October 28, 0830 LT October 29, 1700 LT October 29, and 0230 LT October 30, a water table was established at each site from previously unsaturated conditions throughout the profile (except site 2). Water table elevation moved from undefined within the zone of measurement to approximately 40 cm from the ground surface at site 1 within 8 hours of the start of the storm. Water table position shifted from 50 to 15 cm from the ground surface at site 2 and from undetected to 28 cm from the ground surface at site 3, each within 8 hours. Total potential (ϕ) characteristics prior to the event showed a strongly lateral component. As the event progressed, ϕ

A Rainfall (mm 10 min⁻¹)

B Matric Potential (cm H₂O) — T7, T8, T9, Site 3

C Matric Potential (cm H₂O) — T4, T5, T6, Site 2

D Matric Potential (cm H₂O) — T3, T2, T1, Site 1

E Runoff (mm hr⁻¹) — M8

2400 1200 2400 1200 2400 1200
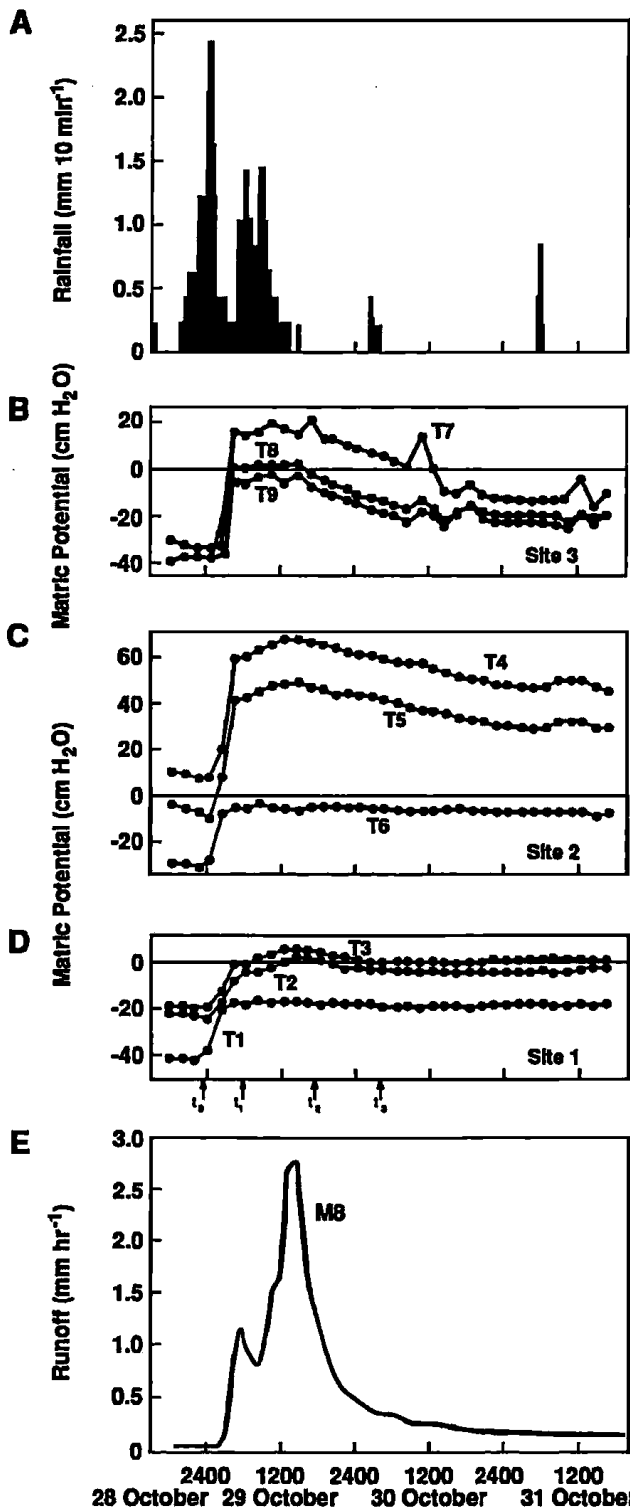28 October 29 October 30 October 31 October

Fig. 4. Hydrometric and tensiometric response for the October 29 event. Precipitation intensity (Figure 4a) and M8 runoff (Figure 4e) are shown for the catchment, in relation to soil physics response at sites 1, 2, and 3 (Figures 4d, 4c, and 4b, respectively). Note rapidity of response and longevity of positive ψ conditions.
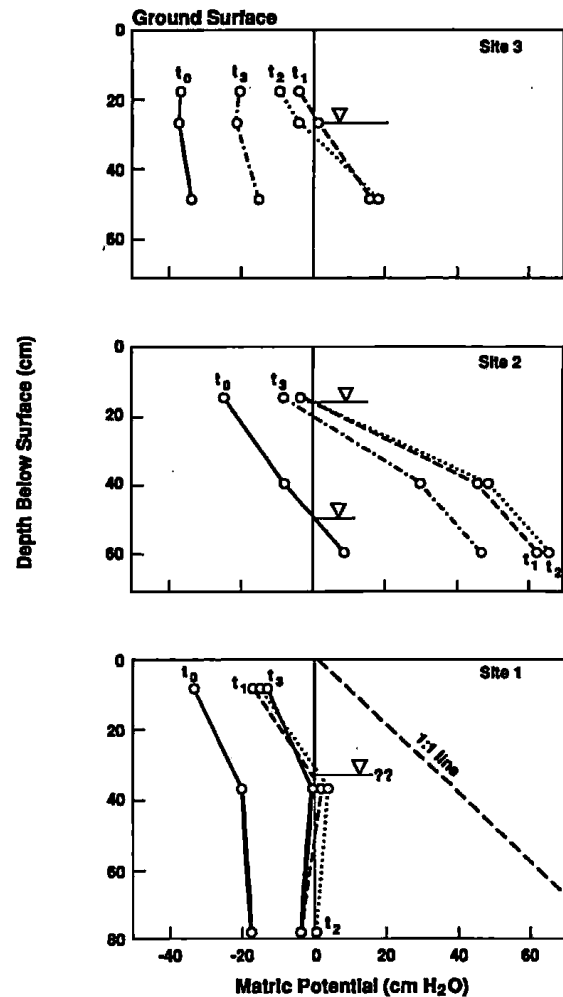
Fig. 5. Near-stream ψ versus depth below surface for the October 29 event.

location [McDonnell, 1989], ψ response to rainfall input was very rapid through the complete profile for each site location, and water tables were quickly established and maintained at depth. Rapid transition from matric to pressure potential occurred generally within 6 hours of the start of the storm and promoted increased downward φ gradients toward the stream channel at site 1. Some lag in ψ response to rainfall input with depth was observed, consistent with the notion of initial downward wetting front propagation through the soil matrix. This pattern rapidly changed to accelerated ψ shift in the lower soil profile, due to perching of groundwater at the mineral soil-Old Man Gravel interface.

Once peak ψ was reached within the profile, values persisted for 1–3 days before gradually returning to prestorm ψ. The maintenance of saturated zones in the near-stream location is a function of the shallow soil cover, underlain by impermeable Old Man Gravels. Additional subsurface flow from upslope zones and low slope angles would also have contributed to persistent low ψ.

4.2. Midslope Response

Tensiometer numbers and porous cup depths for selected tensiometers in the Pit 5 location are shown in Figure 6. The

gradients shifted from lateral to a more downprofile direction (Figure 5). Gradients become more lateral upslope, with downward flow predominating closer to the channel.

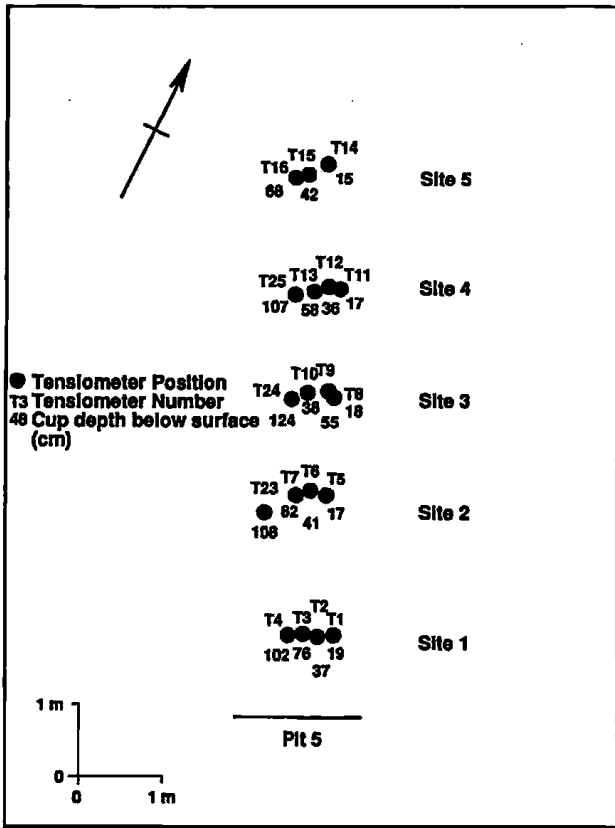In each of the monitored 1987 storms in the near-stream

Fig. 6. Tensiometer numbering and porous cup depths for the Pit 5 midslope site.

October 29 storm (already discussed for the near-stream zone) is discussed in detail, and specific time periods t_0, t_1, t_2, etc. (cited above) will also be used for the following discussion of midslope response to storm rainfall. Pit 5 through-flow rates were not available for this event, so ψ − Q comparisons cannot be made. It is assumed, however, that Pit 5 through-flow timing was roughly equivalent to Pit A (Figure 7f).

Soil water potential response to storm rainfall at Pit 5 was very rapid throughout the profile, and positive ψ was established at the base of the profile at most sites within 8 hours of the start of the event (Figure 7). The midslope site differed in the timing of response, compared with the near-stream location. In this case, ψ response shapes were closely aligned with the main Pit A hydrograph (Figure 5f), exhibiting both a steep rise and recession. In response to the second rainfall burst between 0600 and 1200 LT October 29, sites 1–4 showed an immediate and large shift into positive ψ conditions and with no lag with depth.

At site 1, T1 (19 cm) and T2 (37 cm) reached peak ψ within 3 hours of the first rainfall burst (Figure 7e). A second ψ peak of equal magnitude occurred at 1200 LT, corresponding to the second rainfall burst. T3 (76 cm) and T4 (102 cm) showed no ψ peak in response to the first rainfall burst and only began to respond to the second episode. T3 and T4 rose sharply between 2400 LT October 28 and 1200 LT October 29 and then receded at the same rate for another 12 hours before declining more slowly. Low-magnitude ψ was maintained only briefly, as compared to both the near-stream
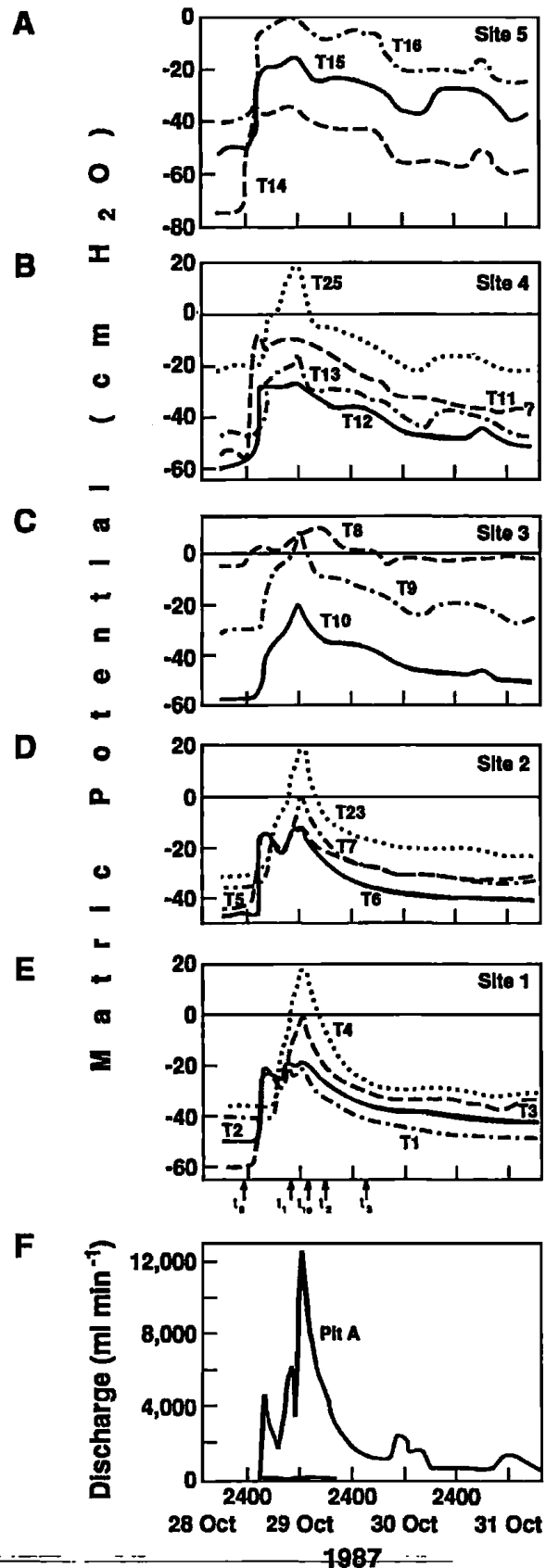
Fig. 7. Hydrometric and tensiometric response for the October 29 event. Pit A throughflow (Figure 7f) is shown in relation to soil physics response at sites 1–5 (Figures 7e–7a, respectively). Note difference in recession of ψ compared to near-stream site.
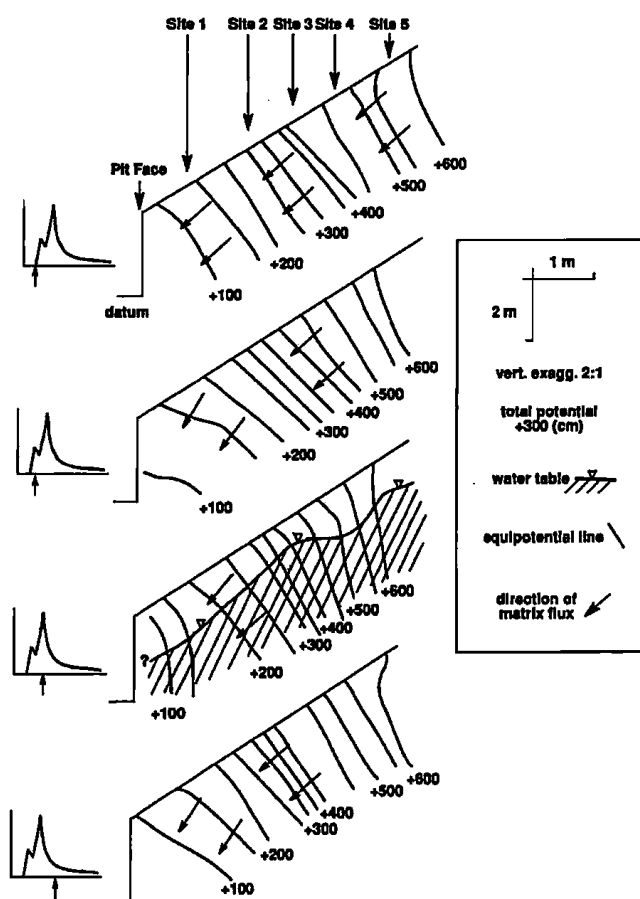
Fig. 8.   Cross-sectional diagram (with 2x vertical exaggeration) for the Pit 5 midslope site, indicating ϕ (in centimeters) and corresponding flow lines for time t_0–t_3 during the October 29 event. Note the fixed datum at the bottom of the Pit 5 face.

conditions and the October 24 event conditions at the midslope site.

Tensiometric response to storm rainfall at site 2 was almost identical to site 1 (Figure 7d). Moving further upslope, peak ψ response at depth was more subdued and showed a rise to peak, followed by constant low-magnitude ψ. The variation in response, particularly at depth, may be a function of a buildup of saturation near the pit face, as described by Atkinson [1978], where a saturated wedge is established upslope of the face. Nevertheless, much of the profile throughout the midslope zone became saturated and maintained positive ψ throughout the catchment's peak runoff response.

Figure 8 shows a very rapid appearance and disappearance of water tables throughout the zone but particularly near the pit face (i.e., sites 1 and 2). Total potential gradients during the October 29 event show a consistent lateral flux component, with some downward flux near the pit face at t_1. The localized downward component shows the effect of the pits' face, but ϕ contours in Figure 8 suggest that for this event at least the influence of the pit may be within about 2 m of the face. Highest ϕ gradients were established at t_{1a} (1200 LT October 29), coinciding with peak ψ and peak pit throughflow. A detectable water table (i.e., somewhere above the deepest tensiometer at each site) was only observed at t_{1a}. This rapid appearance and disappearance of

the water table at depth is very different to the near-stream situation, where water tables persist for some time.

Midslope response was highly variable for other monitored 1987 events of different storm magnitudes, intensities, and prestorm soil ψ conditions [McDonnell, 1989]. Response seemed to indicate a more erratic infiltration-ψ relationship than the near-stream zone. During monitored low-magnitude events of 5–10 mm rainfall, tensiometric data are consistent with a semiconstant wetting front propagation through the profile and with strong ψ response lags with depth. Although some bypass flow seemed to occur in the upper soil horizon (<50 cm), rainfall depth and soil moisture content was low enough so that the lower soil depths did not receive appreciable moisture from above until streamflow response had subsided. Water tables therefore did not develop at the Pit 5 site, and subsurface storm flow volumes were negligible.

During large magnitude events, matric potential in the lower soil horizons (>75 cm) responded almost instantaneously to infiltrating rain. In each storm, elevational potential dominated total potential computations, and total potential gradients were strongly lateral in the downslope direction. Water table longevity was very short (as compared to the near-stream zone) and showed a close correspondence with Pit 5 through-flow rate. Downslope drainage of perched groundwater was extremely efficient and showed no lag with recorded pit throughflow for storms where these data were available.

5. Discussion

5.1. Can Near-Stream Valley Bottom Groundwater Sustain Old Water Storm Flow Volumes?

Tensiometer evidence for the near-stream zone showed that ψ response to rainfall input is rapid, and water tables are quickly established and maintained at depth. Transition from matric to pressure potential occurred generally within 6 hours of the start of the storm and promoted increased downward ϕ gradients toward the stream channel. If the near-stream groundwater ridging mechanism is to explain total catchment runoff, then sufficient volumes of old water must be discharged through this limited near-stream zone to account for measured runoff volumes at the M8 weir. A crude calculation of potential near-stream groundwater flux (q) can be made using measured K_{sat} values from Mosley [1979] along with typical near-stream ϕ values (measured from the near-stream tensiometer plot) and computed channel dimensions:

$$q = -K_{sat}\, d\phi/dL \qquad (1)$$

where q is the flux rate in millimeters per hour and $d\phi/dL$ is the gradient of ϕ toward the channel. Assuming a K_{sat} of 30–300 mm hr^{-1}, and a typical ϕ gradient of 0.67 (from the October 29, 1987, event, McDonnell [1989]), $q = $ 2–20 mm hr^{-1}. If groundwater ridging is important along 125 m of the stream channel (as outlined above) and the saturated depth through which water seeps into the channel is 1 m, then the potential seepage face would be 250 m^2 (assuming water entered from both sides of the channel). Combining the flux rate with the seepage area and then dividing by the catchment area (3.8 ha) produces a near-stream subsurface runoff contribution of 0.13–1.3 mm hr^{-1}. This range of discharge is
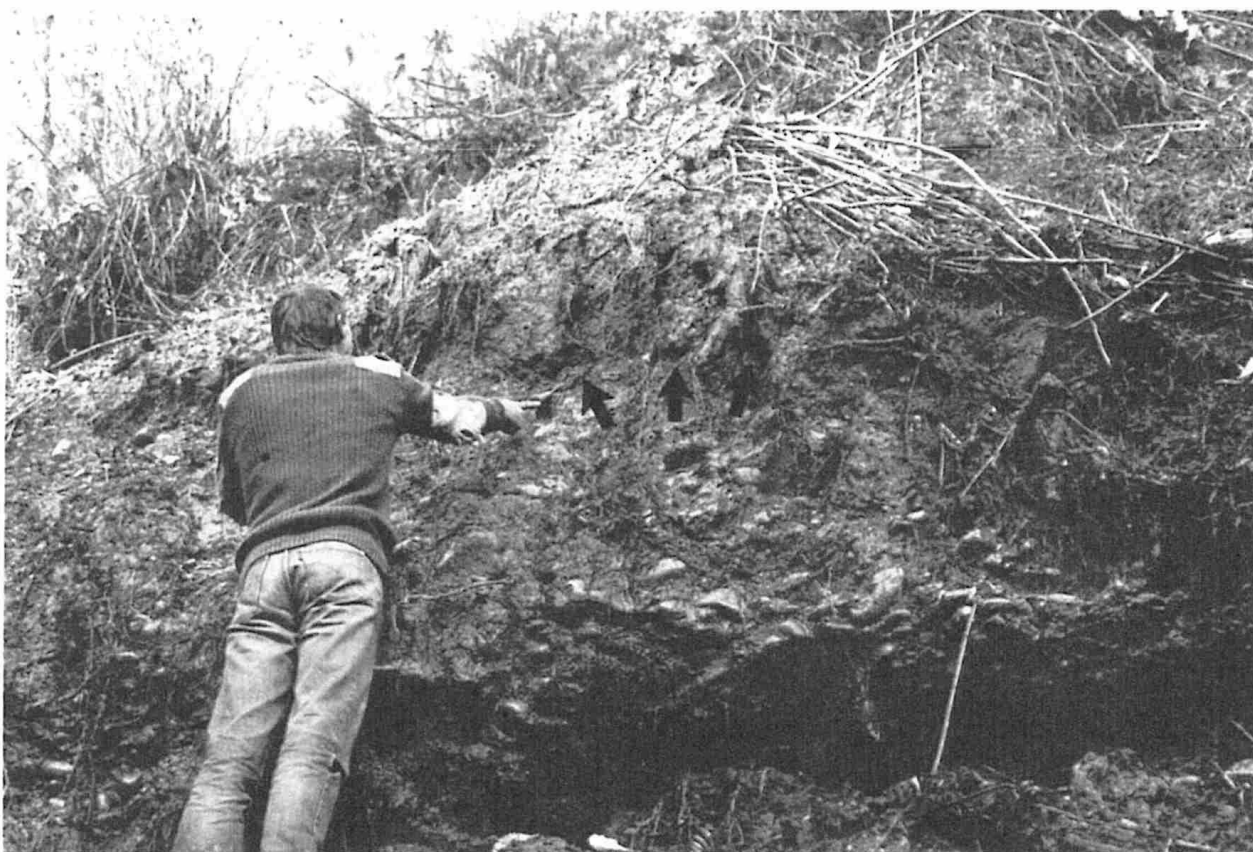
Fig. 9. Photograph of pipes venting to the atmosphere along the bank of a steep first-order channel within the M8 catchment. Soils in these positions simply form a face at which water from upslope hollows drains into channel zones.

sufficient to account entirely for the *Pearce et al.* [1986] April 1979 storm but not for the peak of old water discharge for the *Sklash et al.* [1986] September 7–8, 21–22, and 25, 1983, storms or many of the 1987 storms reported by *McDonnell* [1989]. Although a number of simplifying assumptions have been made, the q value suggests that subsurface flux in near-stream valley bottom locations is important in many (but not all) storms.

For events yielding >2 mm hr^{-1} peak storm flow, hillslope hollow drainage into steeply sloping first-order channels dominated old water production and channel storm flow. These processes are seen as distinctly different to valley bottom near-stream behavior. Zones adjacent to first-order channels were characterized by highly incised, steep-sided banks. In many locations the sloping soil mass simply formed a face at which water seeped into the channel (roughly analogous to a pit face). Figure 9 shows an example of this type of channel section, where macropores at the base of the mineral soil layer issue directly into the channel zone. Although this example is from a newly formed stream section (discussed in detail by *McDonnell* [1990]), it characterizes much of the steep first-order channel zones within M8. Hillslope hydrological processes identified at Pit 5 therefore are assumed to be directly comparable to processes controlling water movement to stream areas within these steep first-order channel zones.

5.2. A Simple Model of Runoff Response

A model for runoff response in the M8 catchment must satisfy two apparently divergent phenomena: (1) runoff production is extremely rapid, with most flow delivered to stream channels via macropores, and (2) the groundwater (old water) component in channel storm flow is in excess of 85% [*McDonnell*, 1989]. The answer to this problem may simply relate to the large soil water store (350–500 mm) relative to rainfall input during individual storms (typically 25–75 mm). *Sklash et al.* [1986] argue that since less than 30% (in their monitored events) of the rainfall amount appears as quick flow, about 70% of the rainfall either infiltrates or is intercepted, and this is sufficient to supply the subsequent low-flow discharge and transpiration until the next storm. Furthermore, only a small amount of the soil water store must be discharged to obtain the quick flow yield in most storms. Tensiometric evidence from the present study shows that much of the catchment is within 10% of soil saturation for most of the year, and prestorm ψ is generally between −20 and −80 cm H$_2$O. Therefore all that is required to satisfy the rapidity of catchment runoff response is an efficient transport system to bring stored water quickly from the hillslopes to the surface channels.

Soil moisture content in the M8 catchment increases substantially in the downslope direction because of steep

slope angles and relatively permeable soils. The near-stream valley bottom zone, along the main channel, represents the only zone of semipermanent aquifer storage, where $\psi > 0$ cm H_2O in the subsoil. During the initial wetting of the profile, available moisture storage in zones closest to the channel is filled, and resident groundwater begins to discharge into the channel, assisted by groundwater ridging (or mounds) along the channel margins. Soil water overlying the near-stream groundwater ($\psi = -20$ to -40 cm H_2O) is rapidly converted to $+\psi$ and is then displaced into the channel. This process is seen as a near-stream subsurface response and would probably only occur in the valley bottom zone of the main channel section. This subsurface near-stream response is in addition to valley floor saturation overland flow and on-channel precipitation.

As the hydrograph starts to rise, near-stream zones along the steep first-order channels would also start to discharge groundwater into the ephemeral channels. The majority of this input would come from hollow zones (small zero-order basins) upslope from the channel bank. Initially, matrix flow from a growing saturated wedge would contribute to channel inflow, but then as perched water table conditions over the Old Man Gravels developed on the slopes, pipes would conduct the majority of saturated flow downslope. Depending on the total depth of rainfall, hollow saturated zones would expand upslope and increase in local saturated zone thickness, feeding a well-connected system of pipes that would transport the water quickly downslope and into the first-order channels. Even if the pipes were not well connected throughout the slope, kinematic theory suggests that transmission of pressure waves downslope may augment hillslope response if the pipes are locally in zones of saturation and flowing full. At the same time, valley bottom near-stream zones would continue to exfiltrate groundwater into the main channel, with increasing contributions from upslope zones.

At peak flow, water table elevations in the near-stream and hillslope hollow zones would be at their maximum level. Once rainfall inputs ceased, hillslope zones would quickly drain via pipe flow, such that hillslope subsurface flow rates would decrease faster than M8 hydrograph recession. This was observed for both the Pit 5 and Pit A plots. The recession limb of the hillslope-only hydrograph would be like that of a sponge; drainage from the pipes would "shut down" as soon as perched water tables in the hillslope hollows are dissipated. The majority of the subsequent stream recession would be fed by valley bottom near-stream zones, whose deeper aquifer storage (and any additional drainage from upslope) would continue to supply the receding limb. Tensiometric data for the near-stream site showed that once peak ψ was reached within the soil profile, values persisted for 1–3 days before gradually returning to prestorm ψ values.

The simplified model follows the Hewlett and Hibbert [1967] notion of an expanding contributing zone through the event and satisfies soil physics data presented earlier. The difference in the two models lies in the mechanism of response, whereby the exceedence of a threshold rainfall depth (and/or intensity) during the hydrograph rising limb converts the system from a matrix-dominated near-stream flux to a pipe flow dominated hillslope hollow system. A reverse switching back to matrix-dominated near-stream flux occurs during the stream recession as soon as perched water

tables on hillslopes are dissipated. Although the response described above is almost entirely old water dominated, some new water input to the channel would be derived from direct precipitation onto the limited near-stream saturated area and from headwater responses.

5.3. A Proposed Mechanism for Macropore Flow of Old Water

The notion of capillary fringe induced groundwater exfiltration observed in many isotopic investigations has been used to explain large old water storm flow volumes. The basis of these claims has come mainly from laboratory study [e.g., Abdul and Gillham, 1984] and numerical simulation [e.g., Sklash and Farvolden, 1979]. This has been a dual result of observations made in the laboratory with repacked "sand box" soils, coupled with the algorithmic convenience afforded by the analytic representation of a capillary fringe in the soil's water characteristic. In the soil physics literature, however, the notion of soil having a tension-saturated zone, or capillary fringe, has been questioned. Field retention data have failed to observe significant zones of tension saturation in clays and loams [Perroux et al., 1982], and Clothier and Wooding [1983] even question the presence of such zones in laboratory media.

The water characteristics presented in Figure 2 indicate that M8 soils release water with any applied suction and as such do not maintain a discrete tension saturated zone or capillary fringe. Although these are in fact release curves, they provide an estimate of the amount of water still in storage at a given ψ and allow an estimate of how much water is required to saturate the soil. Because M8 soils do not have a capillary fringe, they will actually absorb some water during wetting close to saturation. Thus they have some storage capacity. For example, in the near-stream zone, soils are roughly 0.5 m deep, with antecedent ψ of approximately -40 cm H_2O and porosity of 0.66. Thus some 20 mm of rain could be absorbed by the soil, which is in agreement with processes outlined in Figure 4.

At the Pit 5 midslope hollow site, where soil depths and prestorm suctions are more than double those in the near-stream zone, data in Figure 7 indicate that it may be completely unrealistic to assume that these soils wet up nicely along their $\psi(\theta)$ trajectory, as given by their statically determined, equilibrium representation in Figure 2. So there is a conundrum; why do these soils behave as if they have capillary fringe properties (i.e., limited storage), in terms of measured rapid ψ and water table response? It is likely that the appearance of limited storage arises out of disequilibrium in potential during wetting, which is created by soil inhomogeneities or macropores.

Figure 10 illustrates how in steeply sloping hollow zone, bypass flow leads to the soil truly "releasing" water long before wetting along a measured $\psi(\theta)$ would predict, due to pressure potential disequilibrium within the soil. In this discussion it is important to distinguish between the conductivity of the matrix (K^*) and that of the soil with macropores (K_{sat}). If the flux density of rain, Vo, is greater than K^*, local ponding will eventually occur, leading to vertical bypassing (whether or not Vo is greater than K_{sat}). Therefore it is not unrealistic for 5–10 mm hr^{-1} rainstorms to create localized ponding on a soil purported to have a K_{sat} of 100 mm hr^{-1}. It just means that K^*, the appropriate matrix property, is less
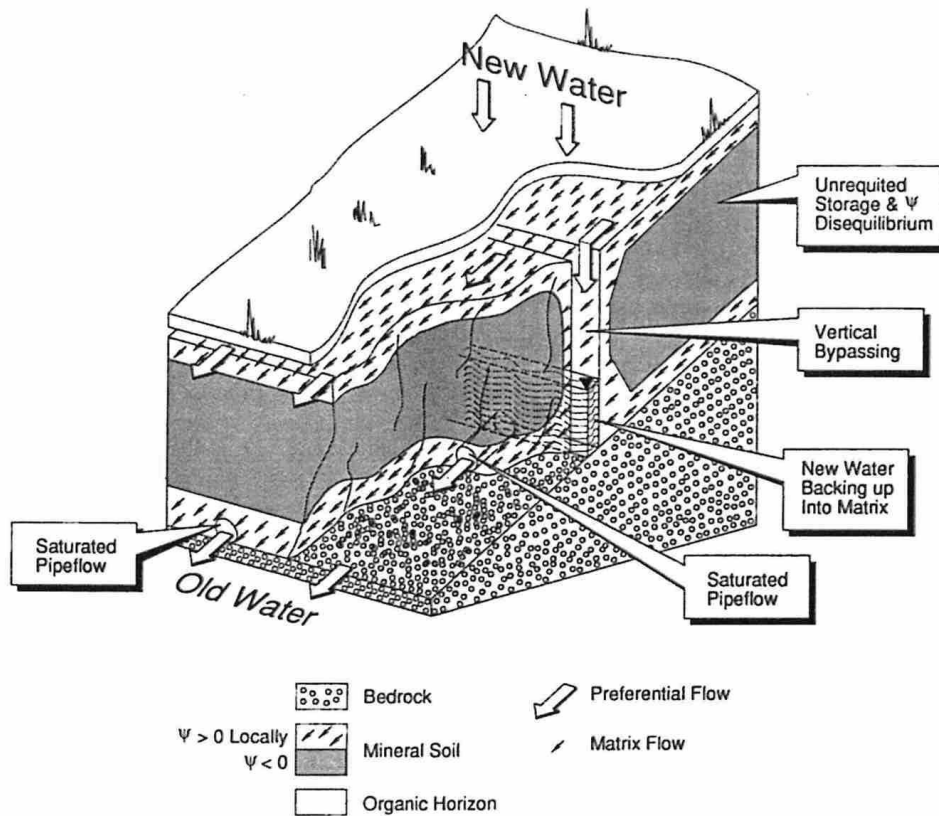
Fig. 10. Conceptual model of runoff production in midslope hollows, combining the idea of unrequited storage and ψ disequilibrium in producing a preferential flow of fully mixed (old) water. In this case, rain flux density exceeds mineral soil surface K^* and moves to depth via vertical cracks. The invading new water perches at the soil-bedrock interface and "backs-up" into the newly saturated matrix. Once free water exists, large pipes in the lower soil zones quickly dissipate transient water tables laterally downslope, producing a rapid through-flow response of well-mixed old water.

than 5–10 mm hr^{-1}. Local bypassing requires minimally that $Vo > K^*$.

During rainfall wetting in the M8 catchment, water infiltrates the organic layer and encounters the mineral soil surface. In some situations [Mosley, 1979; McDonnell, 1989], $Vo > K^*$, and water flows downslope over the mineral soil surface. In areas with vertical cracks (e.g., Pit 5 midslope hollow), free water on the mineral soil surface flows downslope until it encounters a crack and bypasses to depth. The matrix may still have unrequited storage capacity, but soil water diffusion to unsaturated locales is too slow, relative to its preferential drainage via a crack. Uniform wetting and distribution of infiltrating water may be additionally confounded by the soil not uniformly draining to equilibrium potential beforehand and by hydrophobicity developed along crack walls, as described earlier. The cracks may break capillary continuity, thus limiting matrix drainage, leaving crack walls primed to initiate bypass flow at the beginning of the next rainfall episode. Therefore the pseudo-limited storage response observed at Pit 5, for example, may be a consequence of a dynamic, disequilibrium wetting process, whose interpretation is not possible using static, equilibrium $\psi(\theta)$ information.

As invading new water moves to depth, free water perches at the soil-bedrock interface, and "backs-up" into the matrix, where it mixes with a much larger volume of stored old matrix soil water (Figure 10). Pressure potential evidence

from Pit 5 showed that lower-profile tensiometers responded disproportionately, in terms of measured ψ response due to water perching at the mineral soil-bedrock interface. Midslope water tables developed to over 0.5 m of head in the October 29 event. Once established, however, the water table is dissipated by the moderately well-connected system of pipes at the mineral soil-bedrock interface. The relationship between crack infiltration and lateral pipeflow is not linear, because there is a significant time delay between water table perching and subsequent distribution of $+\psi$. This delay is thought to be the key process in shifting new water signatures to that of old water. Isotopic data from Pit 5 through flow [Sklash et al., 1986] showed that old water dominated subsurface flow at these sites by up to 95%. The pipes distribute this mixture of newly bypassed rainfall and mixed stored water downslope to the first-order channel bank. The shift from old water to new water is expected to occur on the slope, as illustrated in Figure 10. M. K. Stewart and J. J. McDonnell (1990) showed that between-storm matrix water varies in age from approximately 1 week at the catchment divide to over 100 days at the main channel margin. Sklash et al. [1986] showed that the amount of old water within subsurface storm flow also increased downslope.

Pit 5 through-flow data [McDonnell, 1989] showed that throughflow is sensitive to changes in rainfall, in that the preferential flow system ceases to be recharged and drains

rapidly once rainfall inputs stop. Even though only a small volume of the soil upslope participates in the runoff episode, both *Sklash et al.* [1986] and *McDonnell* [1989] observed that up to 95% of the water emanating from the Pit 5 face is stored water.

Finally, it should be noted no mention has been made of stemflow effects on bypassing. Rain does not fall directly upon the soil surface where soil physical measurements are made. Rather, it is funneled there by the resident vegetation. These plants may focus the water so that the local flux density of water application to the soil surface may be substantially greater than the recorded rainfall rate. In addition, the focus of this water is at the base of the plant, which is the predominant location of the orifices of plant-engendered macropores. Vegetation may play a critical role in the transmission of rainfall to the surface and its soil transport pathways. Although not specifically studied in this investigation, work is currently underway at the NASA Marshall Space Flight Center to try to quantify these speculations.

6. Conclusions

Although previous studies in this and other catchments have viewed macropore flow processes to be delivery of new water, this study has shown that macropore (preferential) flow can result in old water displacement. In the M8 catchment, valley bottom groundwater can respond rapidly enough to account for the old water component in small storms and hydrograph rising limbs of larger events. However, discharge through this zone cannot satisfy all hydrographs. At high flow rates, hillslope hollow discharge into steep first-order ephemeral channels dominates runoff and old water storm flow volumes. A crack-pipe model for hillslope runoff is needed to explain the storm flow volumes of the appropriate isotopic composition at the catchment outflow. Although not directly applicable to other hydrologic systems, this work shows the value of combining hillslope and stream-oriented approaches, in an effort to improve our understanding of hydrogeochemical fluxes from forested watersheds. Furthermore, continuous three-dimensional recording of soil water potential conditions greatly illuminates the black box of hillslope flow processes.

References

Abdul, A. S., and R. W. Gillham, Laboratory studies of the effects of the capillary fringe on streamflow generation, *Water Resour. Res.*, *20*, 691–698, 1984.

Atkinson, T. C., Techniques for measuring subsurface flow on hillslopes, in *Hillslope Hydrology*, edited by M. J. Kirkby, pp. 73–120, John Wiley, New York, 1978.

Beven, K., Micro-, meso-, macroporosity and channeling flow phenomenoa in soils, *Soil Sci. Soc. Am. J.*, *45*, 1245, 1981.

Beven, K. J., and P. Germann, Macropores and water flow in soils, *Water Resour. Res.*, *18*, 1311–1325, 1982.

Bouma, J., Soil morphology and preferential flow along macropores, *Agric. Water Manage.*, *3*, 235–250, 1981.

Bouma, J., and J. L. Anderson, Relationships between soil structure characteristics and hydraulic conductivity, Field Soil Water Regime, *Spec. Publ. Soil Sci. Soc. Am.*, *5*, 77–105, 1973.

Bouma, J., A. Jongerius, O. Boersma, A. Jager, and D. Schoonderbeek, The function of different types of macropores during saturated flow through four swelling soil horizons, *Soil Sci. Soc. Am. J.*, *41*, 945–950, 1977.

Clothier, B. E., and R. A. Wooding, The soil diffusivity near saturation, *Soil Sci. Soc. Am. J.*, *47*, 636–640, 1983.

Germann, P. F., Rapid drainage response to precipitation, *Hydrol. Processes*, *1*, 3–13, 1986.

Gillham, R. W., The capillary-fringe and its effect on water-table response, *J. Hydrol.*, *67*, 307–324, 1984.

Hewlett, J. D., and A. R. Hibbert, Factors affecting the response of small watersheds to precipitation in humid areas, in *International Symposium on Forest Hydrology*, edited by W. E. Sopper and W. H. Lull, pp. 275–290, Pergamon, New York, 1967.

Jones, J. A. A., Extending the Hewlett model of storm runoff generation, *Area*, *11*, 110–114, 1979.

Jones, J. A. A., The effects of soil piping on contributing areas and erosion patterns, *Earth Surf. Processes Landforms*, *12*, 229–248, 1987.

Luxmoore, R. J., Micro-, meso-, and macroporosity of soil, *Soil Sci. Soc. Am. J.*, *45*, 671, 1981.

McCaig, M., Contributions to storm quickflow in a small headwater catchment—The role of natural pipes and soil macropores, *Earth Surf. Processes Landforms*, *8*, 239–252, 1983.

McDonnell, J. J., The age, origin and pathway of subsurface stormflow in a steep, humid headwater catchment, Ph.D. thesis, 270 pp., Univ. of Canterbury, Christchurch, N. Z., 1989.

McDonnell, J. J., The influence of macropores on debris flow initiation, *Q. J. Eng. Geol.*, in press, 1990.

McDonnell, J. J., M. Bonell, M. K. Stewart, and A. J. Pearce, Deuterium variations in storm rainfall: Implications for stream hydrograph separations, *Water Resour. Res.*, *26*, 455–458, 1990.

Mew, G., T. H. Webb, C. W. Ross, and J. Adams, Soils of Ignangahua Depression, South Island, New Zealand, *Rep. 17*, N. Z. Soil Surv., Christchurch, 1975.

Mosley, M. P., Streamflow generation in a forested watershed, New Zealand, *Water Resour. Res.*, *15*, 795–806, 1979.

Mosley, M. P., Subsurface flow velocities through selected forest soils, South Island, New Zealand, *J. Hydrol.*, *55*, 65–92, 1982.

New Zealand Soil Bureau, General survey of the soils of the South Island, New Zealand, NZ Soil Bur., *Bull. 4*, 404 pp., N. Z. Soil Bur., Wellington, 1968.

Pearce, A. J., and A. I. McKerchar, Upstream generation of storm runoff, in *Physical Hydrology, The New Zealand Experience*, edited by D. L. Murray and P. Ackroyd, pp. 165–192, New Zealand Hydrological Society, Wellington, 1979.

Pearce, A. J., C. L. O'Loughlin, and L. K. Rowe, Hydrologic regime of small, undisturbed beech forest catchments, North Westland, Proceedings of the 3rd Soil and Plant Water Symposium, *Publ. 1-126*, pp. 150–158, N. Z. Dep. of Sci. and Ind. Res., Lower Hutt, 1976.

Pearce, A. J., M. K. Stewart, and M. G. Sklash, Storm runoff generation in humid headwater catchments, 1, Where does the water come from?, *Water Resour. Res.*, *22*, 1263–1272, 1986.

Perroux, K. M., P. A. C. Raats, and D. E. Smiles, Wetting moisture characteristic curves derived from constant-rate infiltration into thin soil samples, *Soil Sci. Soc. Am. J.*, *46*, 231–234, 1982.

Ragan, R. M., An experimental investigation of partial area contribution, *IAHS Publ.*, *76*, 241–249, 1968.

Rowe, L. K., Rainfall interception by a beech-podocarp-hardwood forest near Reefton, North Westland, New Zealand, *J. Hydrol. N. Z.*, *18*, 63–72, 1979.

Scotter, D. R., Preferential solute movement through larger soil voids, 1, some computations using simple theory, *Aust. J. Soil Res.*, *16*, 257–267, 1978.

Sklash, M. G., and R. N. Farvolden, The role of groundwater in storm runoff, *J. Hydrol.*, *43*, 45–65, 1979.

Sklash, M. G., M. K. Stewart, and A. J. Pearce, Storm runoff generation in humid headwater catchments, 2, A case study of hillslope and low-order stream response, *Water Resour. Res.*, *22*, 1273–1282, 1986.

Smettem, K. R. J., S. T. Trudgill, and A. M. Pickles, Nitrate loss in soil drainage waters in relation to bypassing flow and discharge on an arable site, *J. Soil Sci.*, *34*, 499–509, 1983.

Stauffer, F., and T. Dracos, Experimental and numerical study of water and solute infiltration in layered porous media, *J. Hydrol.*, *84*, 9–34, 1986.

Thomas, G. W., R. E. Phillips, and V. L. Quisenberry, Characterization of water displacement in soils using simple chromographic theory, *J. Soil Sci.*, *32*, 32–37, 1978.

Van Stiphout, T. P. J., H. A. J. Van Lanen, O. H. Boersma, and J. Bouma, The effect of bypass flow and internal catchment of rain on the water regime in a clay loam grassland soil, *J. Hydrol.*, *95*, 1–11, 1987.

Webster, J., The hydrologic properties of the forest floor under beech/podocarp hardwood forest, North Westland, M.Sc. thesis, 77 pp., Univ. of Canterbury, Christchurch, N. Z., 1977.

Wilson, C. A., and P. Smart, Pipes and pipeflow in an upland catchment, *Catena*, *11*, 145–158, 1984.

J. J. McDonnell, Department of Forest Resources, Utah State University, Logan, UT 84322.